Life Cycle Assessment of Graphite, Silicon Composite, and SiliconDominant Anodes for LithiumIon Batteries: Environmental Impacts, Uncertainties, and Supply Chain

*Advanced Sustainable Systems*

ADVANCED SUSTAINABLE SYSTEMS
www.advsustainsys.com

RESEARCH ARTICLE OPEN ACCESS

# Life Cycle Assessment of Graphite, Silicon Composite, and Silicon-Dominant Anodes for Lithium-Ion Batteries: Environmental Impacts, Uncertainties, and Supply Chain Considerations

Elisa Ravesio[1] | Valentina Sumini[2] | Laura Genovese[2] | Daniele Versaci[1] | Silvia Bodoardo[1]

[1]Department of Applied Science and Technology (DISAT), Politecnico Di Torino, Turin, Italy | [2]Coesia Engineering Center, Coesia, Bologna, Italy

**Correspondence:** Elisa Ravesio (elisa.ravesio@polito.it)

**Received:** 3 November 2025 | **Revised:** 3 February 2026 | **Accepted:** 5 February 2026

**Keywords:** European supply chain | life cycle assessment | lithium-ion batteries | monte carlo simulation | silicon-based anodes

## ABSTRACT

Lithium-ion batteries (LIBs) are essential for applications from portable devices to electric vehicles, where higher specific energy and energy density drive innovation. As cathode research moves toward cobalt-free formulations, anode development focuses on incorporating silicon into graphite. Although silicon production is more energy-intensive than synthetic graphite, its superior theoretical capacity (4200 vs. 372 mAh $g^{-1}$) reduces the material demand for equivalent electrochemical performance. This study assessed the environmental impacts of producing and testing three anode types, graphite (benchmark, ~350 mAh $g^{-1}$), silicon composite (10% Si, ~400 mAh $g^{-1}$), and silicon-dominant (80% Si, capacity limited at ~1000 mAh $g^{-1}$) using Life Cycle Assessment (LCA) at laboratory scale. Results indicated that introducing silicon leads to lower impacts under the investigated conditions across most of the 18 midpoint categories of ReCiPe 2016 (H). Regarding the carbon footprint, $CO_2$ emissions decreased by about 40% (from 1.33 to 0.79 kg $CO_2$-Eq) for the silicon composite and up to 97% (0.04 kg $CO_2$-Eq) for the silicon-dominant electrode. Sensitivity analysis highlighted the importance of supply-chain conditions: adopting a European electricity mix and shorter transport distances led to additional reductions even at gram-scale production. Overall, integrating silicon and optimizing regional supply chains promoted more sustainable LIB production.

## 1 | Introduction

The dramatic increase in greenhouse gas emissions resulting from human activities is leading to the rise in extreme natural events like tsunamis, floods, and wildfires. To limit the increase in temperature on Earth's surface, the European Green Deal aims to implement policies in favor of reducing emissions, for example, by promoting electricity transport over fossil fuel-based alternatives. Within this context, Europe is investing resources in the development of numerous gigafactories to achieve independence in battery production from non-European countries [1].

**Abbreviations:** LIB, Lithium Ion Batteries; LCA, Life Cycle Assessment; FU, Functional Unit; LCI, Life Cycle Inventory; MCS, Monte Carlo Simulations; G-A, Graphite Anode; SC-A, Silicon Composite Anode; SD-A, Silicon-dominant Anode; EV, Electric Vehicle; LCIA, Life Cycle Inventory Analysis; TRL, Technology Readiness Level; PAA, Polyacrylic Acid; CMC, Carboxy Methyl Cellulose; SBR, Styrene Butadiene Rubber; SiC, Silicon Composite; TA, Terrestrial Acidification; GW, Global Warming; FE, Freshwater Ecotoxicity; ME, Marine Ecotoxicity; TE, Terrestrial Ecotoxicity; FRS, Fossil Resource Scarcity; FET, Freshwater Eutrophication; MET, Marine Eutrophication; CHT, Cancerogenic Human Toxicity; NCHT, Non-Cancerogenic Human Toxicity; IR, Ionizing Radiation; LU, Land Use; MRU, Mineral Resource Use; SOD, Stratospheric Ozone Depletion; PMF, Particulate Matter Formation; POFHH, Photochemical Oxidant Formation: Human Health; POFTE, Photochemical Oxidant Formation: Terrestrial Ecosystem; WC, Water Consumption; EQ, Ecosystem Quality; HH, Human Health; NR, Natural Resources.

Commercial batteries are already widespread in multiple fields, hence the demand for materials involved in production is continuously growing. Regarding the anode side, the copper current collector remains the most impactful component in terms of sustainability compared to the electrochemically active materials [2]. Graphite is the material of choice for the anode thanks to its easy manufacturability and low cost; however, some ethical concerns related to its extraction in some countries and its limited energy density are driving research toward other materials [3]. For this reason, the use of alternative materials, like silicon, aims to improve the volumetric energy density and at the same time enhance the sustainability of the process [4].

Even if research on lithium-ion batteries (LIBs) is still extensive, this technology is progressively approaching its theoretical limits [4]. Nonetheless, multiple and significant efforts are still necessary to improve the sustainability of their production process. In this study, the Life Cycle Assessment (LCA) has been used as a standardized methodology for quantifying the environmental impacts in terms of emissions and resource consumption, for three different anode compositions (graphite, silicon composite, silicon-dominant) [5].

In literature, multiple LCAs on silicon anodes are available, however, a direct comparison of the results is not possible, as these studies use different or, sometimes, unspecified boundary conditions and functional units (FU) [6–13]. Unfortunately, as described by Eracka et al., the omission of these key parameters limits the proper comparison between different electrode chemistries and cell configurations [14]. Thus, the LCA performed in this study aims to partially fill these gaps at laboratory level, creating a deeper connection between electrochemistry and environmental assessment. In line with the United Nations Sustainable Development Goals (SDGs), with specific relevance to Objectives 7, 9, and 12, this study supports the development of more sustainable energy storage technologies by providing an early-stage life cycle assessment of emerging silicon-based anode materials, enabling environmentally informed design choices in LIB research. All the electrodes and the cells were manufactured at laboratory scale, and all the data were carefully collected to guarantee the construction of a Life Cycle Inventory (LCI), based entirely on primary data for the foreground system.

This study aims to serve as a reference study for an LCA fully based on primary foreground data along all the analysis steps, enabling the direct comparison of different anode chemistries: graphite (G-A), silicon composite (SC-A) and silicon-dominant (SD-A), which is still lacking in the literature [15, 16]. The manufactured electrodes were produced at the laboratories of Politecnico di Torino, electrochemically tested and finally assessed through the LCA using two functional units: 1 Ah of anode capacity and 1 kg of anode. The objective of this study was to provide LCA results based on practical electrochemical measurements, instead of calculations based on theoretical values, which led to an overestimation of the performance of these electrodes.

In the first part of the study, the production processes of the three anode types were compared with the ReCiPe 2016 Midpoint (H) method, confirming previous findings that increasing silicon content can reduce the impact of this production stage [7]. In the second part, a prospective LCA was performed to assess how sourcing all materials within Europe could influence the environmental impacts of cell production, highlighting the relevance of supply chain localization [17]. In the third part of the work, Monte Carlo Simulations (MCS) were performed to quantify uncertainty within the performed LCA. Finally, the last part was based on the calculations with the ReCiPe 2016 Endpoint (H) method to perform a more complete calculation.

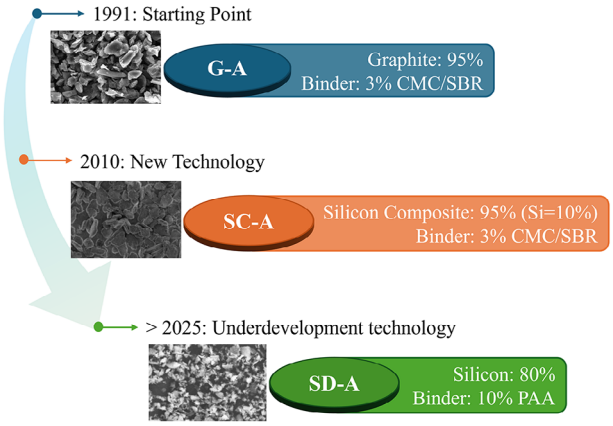


**FIGURE 1** | Conceptual timeline of anode materials used in commercialized LIBs. On the right side are provided additional details about the anode slurry composition used in this work.

## 2 | Methodology

### 2.1 | Goal and Scope definition

Following the guidelines clearly expressed by Scrucca et al., the goal and the scope of this study is to quantify the environmental impact, with a focus on the Carbon Footprint of the production processes of three different types of anodes that contain different amounts of silicon [15]. Although this research approach is not completely new in the LCA field, as some studies have already been published, these analyses typically do not rely entirely on primary data for generating a complete life cycle inventory (LCI) across all individual production steps [7, 9–11, 13].

The anodes examined in this study correspond to different generations of European LIB technology. The first type is a graphite-based anode (G-A) representing Generation 2, which was introduced in commercial LIBs in 1991 and remains the most widely used anode material [18]. Approximately a decade ago, Generation 3a anodes, characterized by the addition of less than 10% silicon, started to be introduced into the market to enhance energy density, is hereafter referred to as silicon composite anode (SC-A) [18]. Looking ahead, Generation 3c anodes, which can incorporate silicon in proportions exceeding 50%, are expected to become prevalent [19, 20]. In this study, silicon-dominant anode (SD-A) with a silicon content of 80 wt.% is selected for this generation (Figure 1), according to promising results reported in previous studies [20, 21]. Further details on the morphology of the investigated materials are provided in Figure S1 and in work [22].

This study also investigates the influence of the functional unit (FU), in accordance with ISO 14040 and ISO 14044 standards and

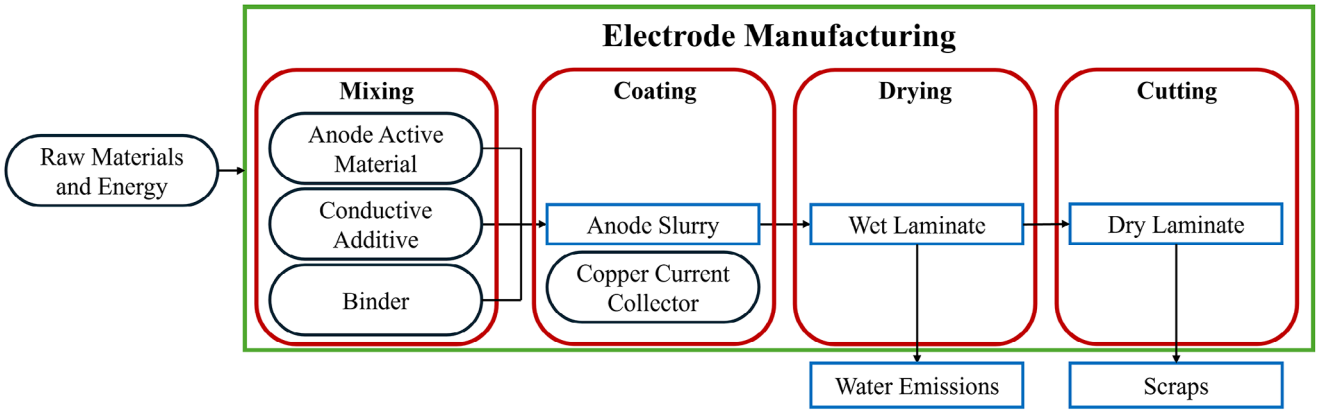


**FIGURE 2** | The system boundary is represented by the green rectangle, while red ovals indicate the production steps. Black ovals represent the materials and components involved in the process as inputs, while blue squares represent the outputs.

consistent with previous studies [15]. When the entire electric vehicle (EV) is assessed, the most used FU is 1 vehicle-kilometer (vkm) [9, 11, 13]. For studies focused on battery packs, common FUs include 1 kWh of storage capacity or 1 kg of battery mass [10, 23]. Similarly, a FU of 1 kg is frequently used for single modules or cells [7]. At a more specific level, although relatively few LCA studies focus only on electrode production, also these studies commonly adopt a mass-based FU (1 kg) [10, 12, 23].

In our study, multiple FUs were employed for the anode production phase. In particular, two FUs were selected: 1 kg of anode produced, aligning with prior assessments, but which limits direct comparison, because of the absence of electrochemical performance [10, 12, 23, 24]. For this limitation, a custom FU of 1 Ah of anode capacity was introduced in this work, becoming particularly relevant when considering the final application of the anodes in full cell configuration. Comparing results based on these two FUs offers a deeper understanding of how FU selection can influence interpretation depending on the study's goal.

The LCA was modelled using the open-source software OpenLCA developed by GreenDelta. The ReCiPe 2016 Midpoint (H) and Endpoint (H) methods were selected for the Life Cycle Inventory Analysis (LCIA) as widely used in the literature, permitting a comparison between the results [7, 9, 10, 23, 25]. Secondary data such as transportation and electricity were obtained from the Ecoinvent 3.11 database.

## 2.2 | System Boundaries and Assumptions

The LCA performed in this work adopts a cradle-to-gate approach (Figure 2), based on the different anode chemistries, using graphite as the benchmark and evaluating the impact of silicon content increment.

An innovative aspect of this study is the evaluation of the environmental impact due to the transportation activities involved in sourcing the raw materials used for coin cell production. Starting from the current global supply chain scenario, a prospective case was developed by modeling a hypothetical supply chain located entirely within Europe. This scenario enables quantification of how transportation distance and associated impacts affect the environmental profile of the production process [25].

Another contribution of this study is the quantification of production scraps. Due to the low technological readiness level (TRL) of the laboratory-scale processes used, the scrap rate was estimated to be slightly below 40%. In contrast, established industrial-scale processes typically achieve scrap rates as low as 5% [26]. This difference is significant and must be considered in any broader evaluation of environmental impact or scale-up potential assessment. Indeed, laboratory scale production is characterized by a huge amount of inefficiency compared to the industrial and most efficient commercial production [16].

Several assumptions were necessary for the LCA modeling process. Since the additive styrene-butadiene rubber (SBR) is not available in the Ecoinvent database, the generic "latex" dataset was used as a proxy during the mixing step. For Polyacrylic Acid (PAA), the dataset for "acrylic acid" was used as the input, while the contribution of the polymeric process was considered negligible, as previously proposed by Nuss et al. [27]. Similarly, for the silicon-carbon composite (SiC) used in this study, which contains 10% silicon, no specific dataset was available; therefore, "silicon carbide" containing 50% silicon was selected as a proxy. For silicon-dominant anodes, metallurgical-grade silicon was selected as a representative proxy for the actual silicon employed, in line with previous work [9]. The water used during the mixing process was assumed to be completely removed during the subsequent drying stage. Moreover, the Italian electricity mix was applied for all energy-related calculations, reflecting the location of the experimental production processes carried out at the laboratories of Politecnico di Torino.

Since all the electrode production processes were performed with water-based binders (both anodes and the cathode), it can be reasonable to assume that for the scale-up process, the impact associated with the strict controlled environment (dry room), which is mandatory for most cathodes, can be significantly reduced [14, 28]. Under such circumstances, only the electrolyte filling step would still require a controlled environment.

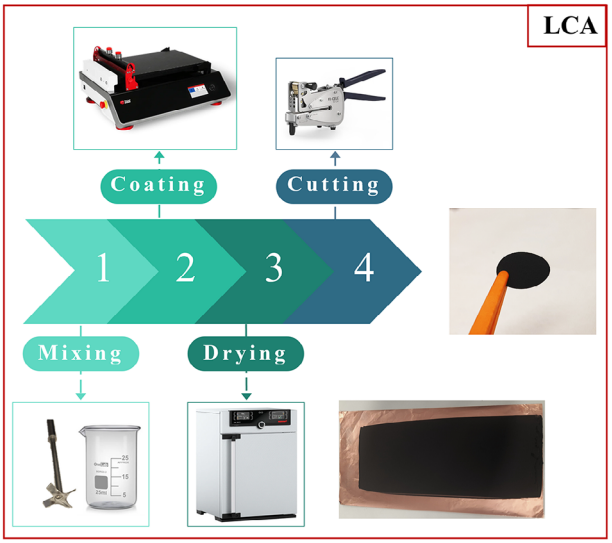


**FIGURE 3** | Summary of the production process starting from the mixing step of the materials, moving through the coating and the drying step to obtain the dried laminate and finally the cutting step to obtain the single electrodes.

## 2.3 | Life Cycle Inventory and Manufacturing Process

The Life Cycle Inventory (LCI) of the electrode production process, developed in this study is based on primary data: the weight of the materials and the electricity consumption were directly collected from the laboratory-scale production. All the other data involved in the LCI, such as raw materials extraction and transformation are complemented with background data from the database Ecoinvent 3.11 Cutoff Unit—Processes. This methodological choice is supported by Carvalho et al. who demonstrated the importance of using primary data for the calculations, comparing two systems, and quantifying the error related to the different types of data chosen [29].

The production process that will be described in this work is a multistep production process, graphically summarized in Figure 3, to finally produce a real coin cell. Initially, three types of anodes G-A, SC-A and SD-A were manufactured using optimized procedures specific to their composition. Subsequently, some electrodes were paired with lithium metal as the counter electrode to measure their practical capacity under operational conditions, ensuring that capacity values reflected realistic use rather than theoretical performance.

For the construction of the complete LCI, a comprehensive set of data related to the power and time of the instruments was collected in Table S1, for the graphite anodes, Table S2, for the silicon composite anodes, Table S3 for the silicon-dominant anodes.

The production process applied in this work aimed to simulate the industrial electrode production process as closely as possible, taking into account the inherent limitations of the facilities involved. A summary of the production steps is reported in Table 1. The process began with mixing all components with the solvent in a multi-step sequence; the wet slurry was then tape-cast onto the current collector and the electrode sheets were dried in an oven. The final step was manual punching of the electrodes into 15 mm discs. A more detailed description of the electrode production process is provided in the Supporting Information.

The electrodes thus prepared were individually weighed, and their thickness was measured to evaluate uniformity of the coating machine: the data are reported in Table 2. In general, the electrodes exhibit certain variations, which are also observed at the industrial level, although in that context the coating quality can be more readily assessed [30].

As mentioned before, the electrodes were tested to measure the practical capacity, as was done by Philippot et al. [9]. The configuration was coin cell 2032 (Figure 4A), further details about the testing conditions are available in the Supporting Information. The electrochemical results obtained from testing these materials are reported in Figure 4B, with additional electrochemical data in Table 3. The instrumentally measured practical capacities were 1.684 mAh for G-A, 2.913 mAh for SC-A, and 4.016 mAh for SD-A. Normalizing these values by the amount of active material yielded specific capacities of 350 mAh $g^{-1}$ for G-A, 400 mAh $g^{-1}$ for SC-A, and 1000 mAh $g^{-1}$ for SD-A (Figure 4B). The corresponding volumetric capacities, calculated from the measured practical capacities and electrode volumes, were 20.79 mAh $cm^{-3}$ for G-A, 33.10 mAh $cm^{-3}$ for SC-A, and 61.78 mAh $cm^{-3}$ for SD-A. As expected, these results confirm that increasing the silicon content in the electrodes enhances performance by improving the final volumetric capacity of the batteries. Additional details on the electrochemical performance of the investigated materials are provided in the Supporting Information.

## 2.4 | Life Cycle Impact Assessments

To ensure consistency with existing literature, the ReCiPe 2016 Midpoint Hierarchist (H) method was selected, as it is widely applied in LCA studies of LIBs [7, 9, 10, 23, 25]. The quantification of impacts across 18 categories enables higher transparency and reduces uncertainties when comparing alternative material systems at an early stage of development [25]. All 18 impact categories provided by the method are reported, while the most representative impact categories are further discussed. The Hierarchist perspective provides a balanced consideration of both short- and long-term environmental effects. Given that the materials investigated include non-commercial and exploratory anode formulations, midpoint indicators allow a more robust and interpretable comparison of environmental trade-offs associated with material production and processing.

In addition, a complementary evaluation using the ReCiPe 2016 Endpoint Hierarchist (H) method was performed to provide a more aggregated and intuitive overview of global impacts. This approach aggregates midpoint categories into three damage categories: Ecosystem Quality (EQ), Human Health (HH) and Natural Resources (NR) [25]. While endpoint indicators can support broader interpretation and decision-making perspectives, they rely on additional modeling assumptions and damage pathways that may increase uncertainty when applied to emerging technologies, and are therefore used here as a complementary rather than a primary assessment [31].

**TABLE 1** | Steps involved in the production process of the electrodes, more information are provided in the Supporting Information.

| | G-A | SC-A | SD-A |
|---|---|---|---|
| Mixing | Time: 210 min | Time: 210 min | Time: 80 min |
| | Rpm: 2200 | Rpm: 2200 | Rpm: 1000 |
| Coating | Time: 10 min | Time: 10 min | Time: 10 min |
| Drying | Time: 60 min | Time: 60 min | Time: – |
| | Temperature: 50°C | Temperature: 50°C | Temperature: RT |

**TABLE 2** | Characteristics of the electrodes depending on their chemistry.

| Chemistry | Solid Fraction (%) | Wet Thickness Deposition (µm) | Dry Layer Thickness (µm) | Dry Layer Volume ($cm^3$) | Weight (mg) |
|---|---|---|---|---|---|
| G-A | 40 | 100 | 46 ± 1 | 0.081 | 15.47 ± 1.60 |
| SC-A | 50 | 100 | 50 ± 1 | 0.088 | 16.09 ± 0.35 |
| SD-A | 60 | 50 | 37 ± 5 | 0.065 | 14.94 ± 0.60 |

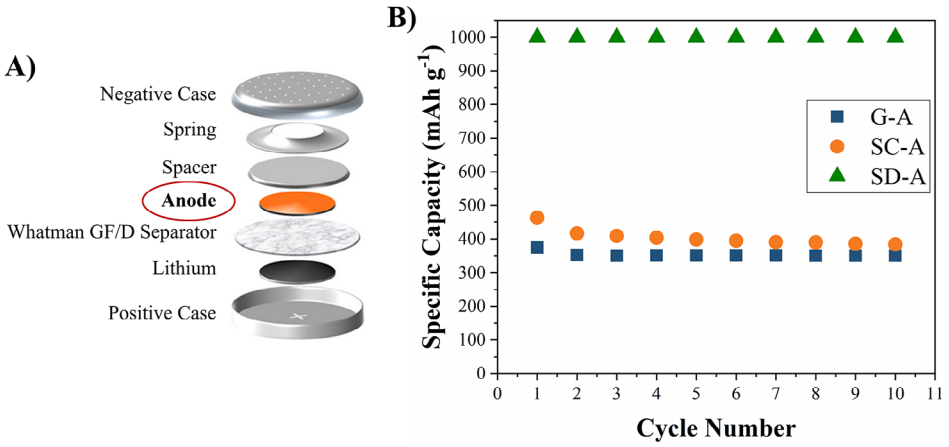


**FIGURE 4** | (A) Coin-cell components for the material testing; (B) Electrochemical results of the electrodes produced for this LCA: half-cells with the anode materials tested versus lithium.

## 2.5 | Sensitivity Analysis

The sensitivity analysis was partially based on the approach proposed by Lavigne Philippot et al. and investigates in more detail the impact of the supply chain [9]. As is widely known, many of the materials required for battery production currently originate from China and, more generally, from Asia [32]. Strengthening the European supply chain could therefore significantly reduce the Global Warming impact associated with battery production.

In the context of rapidly growing demand for electric transportation, the European Union has introduced the European Critical Raw Material Act with the aims of strengthening the EU's strategic autonomy by enhancing the resilience, sustainability, and diversification of supply chains for critical raw materials [33]. Several studies in the literature have explored the supply chain impacts of LIBs at different levels, focusing either on the extraction and processing of specific elements such as graphite, cobalt, and manganese, or on the influence of manufacturing

**TABLE 3** | Electrochemical data measured in the experiments: The practical capacity is the value measured with the instrument, the volumetric capacity is calculated from the practical capacity and the volume of the electrodes.

| Chemistry | Practical Capacity [mAh] | Practical Capacity [mAh $g^{-1}$] | Volumetric Capacity [mAh $cm^{-3}$] |
|---|---|---|---|
| G-A | 1.684 | 350 | 20.79 |
| SC-A | 2.913 | 400 | 33.10 |
| SD-A | 4.016 | 1000 | 61.78 |

location on the battery production process [24, 34, 35]. In particular the study of Philippot et al. highlighted that the electricity mix, and consequently the production country, can significantly affect the global warming potential related to the battery production process [24]. However, to the best of the authors' knowledge, the potential benefits of a fully European supply chain for LIBs have not yet been comprehensively evaluated.

In this study, a single sensitivity case was analyzed in which the supply chain was assumed to be entirely European. The baseline scenario reflected the actual situation, where most materials (graphite, silicon composite, carbon black, CMC, SBR, current collectors and cell components) were sourced from outside Europe. In the prospective scenario, the same materials were assumed to be supplied by European producers. Accordingly, transportation processes were modeled using the Ecoinvent database, which provides data derived from Eurostat, the official European statistical office [36].

It is important to note that this sensitivity analysis accounts only for transportation routes and does not consider potential variations in production processes. Nevertheless, the results indicate that strengthening the European supply chain could substantially reduce the global warming impacts of battery production, not only due to shorter transport distances but also because of the higher share of renewable energy in the European electricity mix compared with countries such as China. This aspect has also been underlined in the study of Philippot et al. [24].

### 2.6 | Data Quality and Uncertainty Quantification Using a Pedigree Matrix

In line with the approach of Philippot et al., this study evaluates uncertainties through the use of a Pedigree matrix, a system that allows the quantification of uncertainty even in the absence of explicit statistical values such as standard deviations [9]. The Pedigree approach distributes uncertainties across five independent categories, each assigned a score between 1 and 5, where 1 represents the lowest uncertainty and 5 the highest. In the Ecoinvent Data Quality System the indicators are Reliability, Completeness, Temporal Correlation, Geographical Correlation and Further Technology Correlation.

Quantification of uncertainties remains a relatively underdeveloped aspect of LCA. Although Igos et al. proposed a more structured framework for uncertainty evaluation, many LCAs do not explicitly report it, particularly in studies of emerging technologies, where uncertainties are often overlooked [37].

In this work, owing to comprehensive data collection, primary foreground data were not associated with uncertainties, as they were directly measured during electrode and cell preparation. Greater attention was therefore placed on the background data. For electricity and transportation, all distributions were assumed to be lognormal, and the geometric standard deviation was calculated based on the Pedigree matrix factors. Uncertainties in electricity consumption were minimized because consumption was measured directly, with precise knowledge of instrument power and operation times; nonetheless, some uncertainty remains due to fluctuations in electricity supply. Transportation data were subject to greater uncertainty, as only partial information on suppliers was available and exact conditions were unknown; consequently, background uncertainties from the Ecoinvent database were adopted as representative values. These uncertainties had the strongest influence on the part of the study assessing the prospective European supply chain.

Uncertainties on global warming (GW) were evaluated through MCS with 10,000 iterations, following the approach adopted in similar studies, as this provides a good balance between result quality and computational time [9, 37]. The MCS allow for the identification of mean and median values: the greater their deviation from the deterministic value, the higher the impact of the uncertainties.

### 2.7 | Criticism and Limitations

It is worth noting that possible limitations of this study are mainly linked to the Technology Readiness Level (TRL) of the processes considered. In fact, all experiments presented here were conducted at a laboratory scale, and the results cannot be directly extrapolated to industrial conditions, where production is generally more efficient and emissions per unit output are lower. For example, estimates for gigafactory-scale production suggest considerably lower impacts than those observed in pilot or laboratory lines [38]. Nonetheless, similar environmental trends are expected at a larger scale due to the inherently more efficient processability of silicon-dominant anodes.

Another important limitation is the adopted system boundary. As a cradle-to-gate LCA, this study does not include the use phase or end-of-life stage. This choice is justified by the fact that the coin cells were fabricated exclusively for research purposes and not intended for commercial applications. The use of the coin cell configuration is mainly motivated by its ease of assembly, which allows precise control of each fabrication step. This manual assembly also ensures higher reproducibility within laboratory scale experiments, although still limited by operator variability. Furthermore, coin cells are not the dominant industrial format, as cylindrical and prismatic cells are more widely employed in the automotive sector and pouch in portable devices. In addition, LCAs on lithium coin cells remain poorly explored in the literature and are typically used only as benchmarks for comparing new technologies, such as solid-state Li-S and Na-ion with the currently most common of Li-ion chemistry [39].

The very small quantities of material involved, often just a few grams or fractions of grams, also represent a limitation, making direct comparisons with industrial-scale studies more challenging. However, even though the materials are processed in small quantities, as typical of university laboratory conditions, the results of this work can serve as a valuable starting point for future upscaling analyses and for bridging the gap between laboratory and industrial production. This limitation is particularly evident in the prospective European supply chain scenario, where variations in environmental impact are present but small, highlighting

that supply chain effects remain relevant even for minor transport quantities.

Finally, limitations arise from the database itself: although Ecoinvent is one of the most widely used and regularly updated databases, some datasets remain outdated. For instance, data related to EURO6 Lorry transportation, the most recent still reference values from the 2013 update, while the dataset for European production of carboxymethyl cellulose states that calculations are based on "average technology from the mid 90s." These examples highlight the challenges inherent in obtaining fully representative LCI data and show how database limitations can influence the accuracy of LCA results.

## 3 | Results and Discussion

The results of the life cycle assessment are presented in the following sections, addressing first the production of anodes, then the impacts of a European supply chain, and finally the uncertainty analysis performed through MCS. This comprehensive framework enables a consistent and robust comparison among graphite-based (G-A), silicon composite (SC-A), and silicon-dominant (SD-A) anodes, under both mass- and performance-based functional units.

Increasing the silicon content to 80% in the SD-A provides advantages not only in terms of specific capacity, leading to higher energy density at full-cell level, but also in terms of material processability, enabling faster mixing and drying steps. The optimization of these processes significantly reduces electricity demand during the production phase, thereby contributing to an overall improvement in environmental performance.

Although most of the materials used in this study were sourced outside Europe, with the exception of silicon supplied by E-Magy, located in the Netherlands, a prospective scenario assuming a fully European supply chain is developed to assess the influence of geographical relocations on environmental impacts [40]. This scenario highlights the relevance of transportation impacts, even for relatively small material flows, while also emphasizing the benefits associated with shorter supply routes and cleaner regional energy systems.

The superior electrochemical performance of silicon-based electrodes implies that smaller quantities of active material are required to achieve comparable capacity, directly translating into lower environmental impact across all impact categories. Furthermore, most of the materials currently used in battery manufacturing are imported from China, where the energy mix is still dominated by coal (around 60%) while renewables account for less than 35%. Although the situation is gradually improving, it still contrasts sharply with the European context, where renewable sources contribute nearly 50% of total electricity generation and coal combustion less than 11% [41]. Consequently, even though silicon production is an energy-intensive process, its overall environmental impact is substantially mitigated when manufacturing occurs within Europe [7, 10]. The sensitivity analysis confirms that adopting a fully European supply chain not only reduces transportation-related impacts due to shorter distances but also decreases production-related impacts owing to the cleaner electricity mix.

When considering the production of 1Ah of electrodes, the number of laminates required highlights the advantage of silicon-rich anodes. Approximately 594 electrodes with a diameter of 15 mm of G-A (equivalent to 7.9 laminates) are needed, compared to 343 electrodes of SC-A (4.6 laminates) and only 249 electrodes of SD-A (3.3 laminates). The lower number of laminates required to achieve the same capacity reduces both production time and waste generation.

In contrast, for the 1 kg functional unit, the material requirements are significantly larger. To produce 1 kg of G-A or SD-A electrodes, around 933 laminates are needed, corresponding to almost 70,000 electrodes per chemistry. SC-A electrodes, being heavier, require fewer pieces, about 62,150 electrodes, equivalent to 829 laminates. These differences in scale highlight how FU choice strongly influences interpretation.

The percentage contribution of individual anode components, presented in Figure 5 and Table S4, reveals a clear trend across chemistries. For G-A (Figure 5A), the copper current collector dominates most categories, often exceeding 90% of the total impact, except in fossil resource scarcity (FRS), where the petroleum-based SBR binder is particularly significant. Mineral resource use (MRU) is almost equally driven by graphite itself and by copper current collector, as the synthetic graphite considered in the Ecoinvent database is produced via the Acheson process, which uses petroleum coke. For SC-A (Figure 5B), the silicon carbide precursor becomes the major contributor across multiple categories due to its highly energy-intensive production process. Similarly, for SD-A (Figure 5C), the dominant influence comes from silicon production, which is predominant over other materials despite the higher share of binder (PAA) used for this system [10].

All the anode components are included and divided between active material, conductive additive, binders and current collector. In G-A, the copper current collector is among the most impactful components across categories, whereas its contribution is less pronounced in silicon-based electrodes, where the silicon production process becomes the dominant contributor. In addition, further considerations can be made: for G-A the FRS impact category is characterized by a not negligible percentage of all the other components, in particular, the SBR is a petroleum-based material which has the greatest contribution for the binder's section. For the SC-A type of anode, the impact of the silicon carbide production is more evident, with its high contribution in more categories, this effect can be mainly attributed to the most energy-intensive production process of the silicon carbide compared to the graphite. A similar interpretation can be done for the SD-A percentage contribution, where silicon production becomes once again one of the most impactful processes.

The contribution analysis excluding current collectors (Figure 5; Table S5) reinforces these trends. For G-A (Figure 5D), the contribution of each component varies across impact categories: for TA and GW, which are mainly driven by electricity production, the contributions are more evenly distributed. For the FRS, the contribution of the conductive additive exceeds that of the active

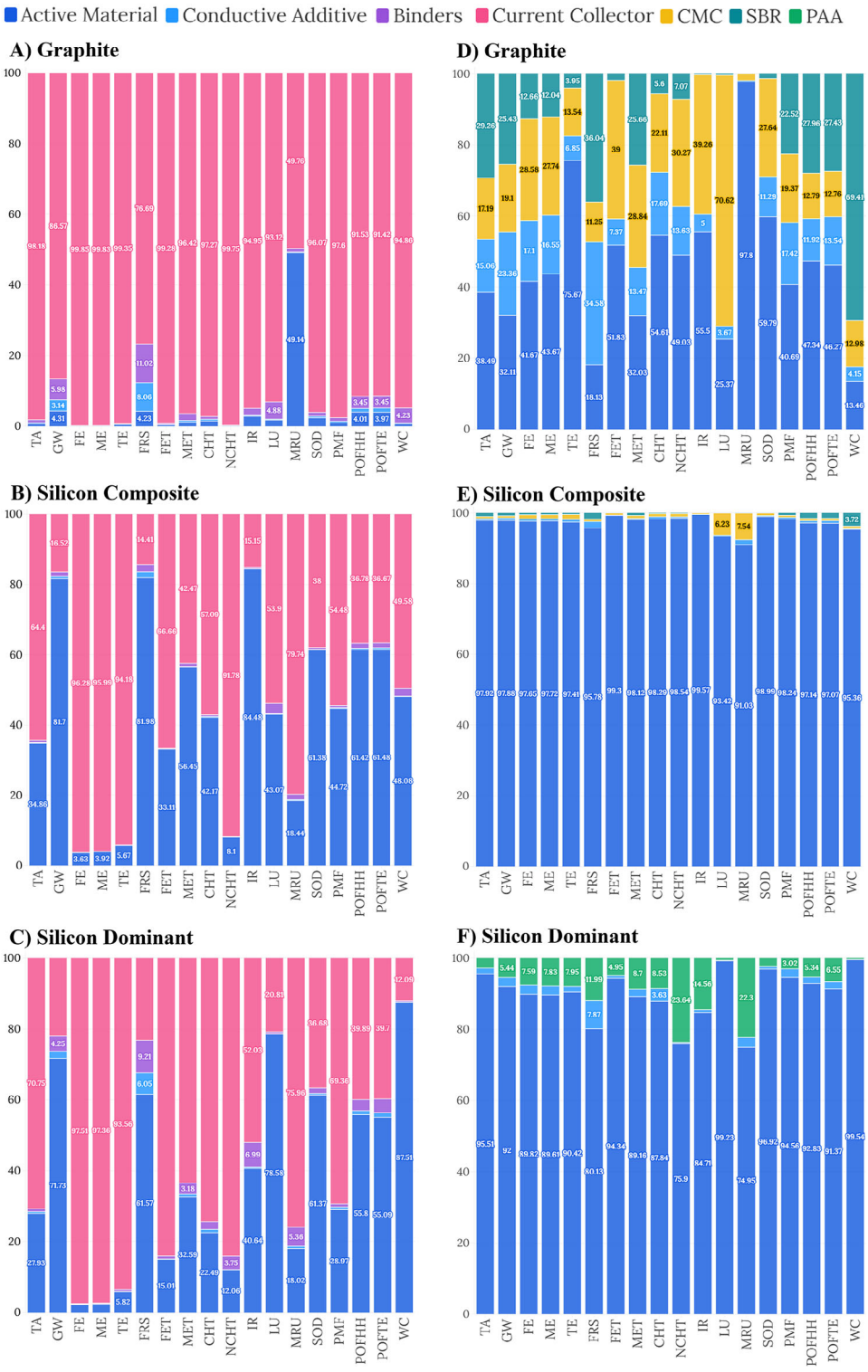


**FIGURE 5** | (A–C) Percentage contribution of the anode components, including active material, conductive additive, binders and current collector: (A) Graphite; (B) Silicon Composite; (C) Silicon-Dominant. (D–F) Percentage contribution of the anode components excluding current collector, including active material, conductive additive and distinguish between binders: (D) Graphite; (E) Silicon Composite; (F) Silicon-Dominant. This percentage impact is the same for the two functional units (1Ah and 1 kg).

material, despite its smaller proportion, and is comparable to that of SBR due to their shared petroleum-based precursors. In the case of MRU, which is the impact category that considers the use of mineral resources, the greatest contribution is from graphite itself. For the LU, the main contribution is the CMC, whose production process is based on some wood-containing pulps, which are chemical treated to obtain some specific characteristics, but the main responsible is still from the agricultural sector. Both for the SC-A (Figure 5E) and for SD-A (Figure 5F), the contribution of the silicon materials is so high that the other

contributions are almost negligible, especially for the SC-A. In case of the SD-A the PAA presents some contributions to the impacts also because it is added in higher percentages compared to the other binders (10% instead of 1%–2%). In addition, the acrylic acid monomer originates entirely from fossil resources, and the use of catalytic materials from mineral resources in its production process significantly contributes to the MRU and MRS categories.

Considering these values, in the following sections the impacts calculated will be described and discussed in more detail.

### 3.1 | Environmental Impact of the Production of 1Ah of Anodes

After the production and the testing of the three types of anodes, their Midpoint impacts were calculated based on the ReCiPe 2016 Midpoint (H) method and the results per each impact category are reported in Table 4. As previously mentioned, across all the impact categories, the presence and increasing content of silicon in silicon-based anodes enhanced electrochemical performance, thereby reducing the number of electrodes needed to achieve 1Ah and consequently lowering the associated impacts. Considering the G-A as the baseline, the percentage reduction was calculated to be between 38% to 42% for the SC-A, while for the SD-A the reduction was substantial, with values between 82% and 97% (Figure 6A,B).

This significant reduction is attributable to two factors: the smaller quantity of materials required to achieve the same electrochemical performance, and the European-based production process of the SD-A. This results from the higher electrochemical capacity of silicon compared with G-A and SC-A, which reduces the number of electrodes required to achieve the same performance, and from the optimized SD-A production process, which minimizes the mixing procedure and eliminates the drying step. In this case, the reliance on renewable resources in the European energy mix clearly demonstrates that favoring such electricity sources can significantly improve the overall sustainability of the process.

Starting from TA, the G-A had an impact of 0.003093 kg $SO_2$-Eq, the SC-A had 0.001862 kg $SO_2$-Equation (−40%) and the SD-A had a value of 0.000196 kg $SO_2$-Equation (−94%). The main contributor processes in this category are mining and metallurgic activities, with copper current collector as the primary driver.

Regarding the GW, the impact of the G-A was 1.33 kg $CO_2$-Eq, while for SC-A was 0.79 kg $CO_2$-Equation (−41%) and for SD-A was 0.04 kg $CO_2$-Equation (−97%). The main contributor of this category is the energy consumed during the production phase. The substantial reduction observed for SD-A reflects its simplified production process, characterized by faster mixing, elimination of the drying step, and reliance on the European electricity mix for silicon production.

TE showed a stronger decrease, from 1.42 kg 1.4-DCB-Eq to 0.84 kg 1.4-DCB-Equation (−41%) for SC-A and to 0.25 kg 1.4-DCB-Equation (−82%) for SD-A. The ecotoxicity impacts are mainly due to the mining process, thus, even though the recycling step was not considered in this study, M. Lavigne Philippot et al. described that all the ecotoxicity impacts can be further reduced when the mining process are avoided [9]. Hence, to generally improve the sustainability of this process, recycled materials should be preferred to reduce the impacts on ecotoxicity.

In case of the FRS, the value for the G-A was 0.431 kg oil-Eq, for the SC-A the value was 0.255 kg oil-Eq and for SD-A was 0.012 kg oil-Eq. The percentage reduction was 41 and 97% for SC-A and SD-A, respectively. In this case, the main contributor to this impact is the SBR, for its petroleum-based origin. In Figure 5 shows that its contribution accounts for nearly half of the total FRU, indicating that its impact is significant and that the development of innovative, bio-based binders should be pursued.

Regarding the LU the G-A presented an impact of 0.028 $m^2$*a crop-Eq, the SC-A reduced this impact at 0.017 $m^2$*a crop-Eq meaning a percentage decrease of 41%. While for the SD-A the impact was reduced to 0.002 $m^2$*a crop-Eq, with a percentage reduction of 93%. The main responsible for this category is the CMC because it is originated from wood-containing pulps, which are directly produced in the agricultural sector.

For the MRU the G-A produced an impact of 0.0163 kg Cu-Eq, the SC-A an impact of 0.0089 kg Cu-Equation (−45%) and the SD-A a reduction up to 0.0009 kg Cu-Equation (−95%). As for the other categories (Figure 5), the copper current collector is the main responsible for this type of impact for all the types of anodes considered. However, in case of the G-A, its impact (49.76%) is almost the same as the graphite (49.18%). This effect is not evident for the silicon-based anodes: in fact, in case of the SC-A the silicon composite impact for the 18.44% and in the case of the SD-A the impact is 18.02%. The resources required for the production of graphite, even if it is synthetic like the one used in this work, have a great impact on the MRU, due to its production process, based on the Acheson process, as declared in the Ecoinvent database.

### 3.2 | Environmental Impact of the Production of 1 kg of Anodes

When normalized to the functional unit of 1 kg of anode produced, the overall impacts are considerably higher than those for the 1 Ah functional unit, reflecting the substantially greater material requirements (Figure 6C,D).

Table 5 reports the impact of values and corresponding percentage reductions compared with graphite-based anodes. Overall, the trend is consistent with that observed for the 1 Ah FU: increasing silicon content reduces environmental impacts, although the magnitude of this reduction varies.

As previously reported by Vijara et al. [7] the addition of 10% or less of silicon is not enough to observe a noticeable effect on environmental impact. In fact, for the SC-A, which contains only 10% of silicon, the reduction compared to G-A is relatively small, typically below 10%, with the notable exception of mineral resource use (MRU), where the reduction reaches approximately 15%. For the SD-A, containing 80% silicon, the reductions are much more significant across most categories, with values between 58% and

**TABLE 4** | Life cycle environmental impacts calculated for the actual production of 1Ah of different types of anodes.

| Impact category | Unit | Results per 1 Ah of production | | |
|---|---|---|---|---|
| | | Graphite | Silicon Composite | Silicon-dominant |
| Acidification: terrestrial (TA) | kg $SO_2$-Eq | 0.003093 | 0.001862 | 0.000196 |
| Climate change (GW) | kg $CO_2$-Eq | 1.334065 | 0.792770 | 0.040852 |
| Ecotoxicity: freshwater (FE) | kg 1,4-DCB-Eq | 1.236692 | 0.766139 | 0.505038 |
| Ecotoxicity: marine (ME) | kg 1,4-DCB-Eq | 1.478156 | 0.915604 | 0.602320 |
| Ecotoxicity: terrestrial (TE) | kg 1,4-DCB-Eq | 1.421925 | 0.839153 | 0.251907 |
| Energy resources: non-renewable, fossil (FRS) | kg oil-Eq | 0.431055 | 0.255443 | 0.012012 |
| Eutrophication: freshwater (FET) | kg P-Eq | 0.000329 | 0.000198 | 1.89E-05 |
| Eutrophication: marine (MET) | kg N-Eq | 3.00E-05 | 1.80E-05 | 1.10E-06 |
| Human toxicity: carcinogenic (CHT) | kg 1,4-DCB-Eq | 0.122757 | 0.073376 | 0.005570 |
| Human toxicity: non-carcinogenic (NCHT) | kg 1,4-DCB-Eq | 1.008620 | 0.600234 | 0.165588 |
| Ionizing radiation (IR) | kBq Co-60-Eq | 0.178266 | 0.105477 | 0.004144 |
| Land use (LU) | $m^2$*a crop-Eq | 0.028259 | 0.016668 | 0.001979 |
| Material resources: metals/minerals (MRU) | kg Cu-Eq | 0.016292 | 0.008966 | 0.000873 |
| Ozone depletion (SOD) | kg CFC-11-Eq | 6.01E-07 | 3.53E-07 | 1.83E-08 |
| Particulate matter formation (PMF) | kg $PM_{2.5}$-Eq | 0.001196 | 0.000728 | 6.94E-05 |
| Photochemical oxidant formation: human health (POFHH) | kg $NO_x$-Eq | 0.002088 | 0.001250 | 8.83E-05 |
| Photochemical oxidant formation: terrestrial ecosystems (POFTE) | kg $NO_x$-Eq | 0.002231 | 0.001335 | 9.34E-05 |
| Water use (WC) | $m^3$ | 0.018098 | 0.010571 | 0.000990 |

90%, although freshwater and marine ecotoxicity (FE and ME) show more modest improvements. This could be related to the silicon production process which is the most impactful process along the supply chain [10].

Considering the GW, the G-A presents a high emission of 157 kg $CO_2$-Eq, which are partially reduced to 143 kg $CO_2$-Equation (−9%) for the SC-A and dramatically reduced to 11 kg $CO_2$-Equation (−93%) for the SD-A, confirming the advantage of the silicon-dominant chemistry in reducing carbon emissions per unit of electrode mass.

Moving toward the ecotoxicity impacts, for the FE and the ME the trend reversed compared with the 1Ah FU. G-A recorded 145.6 kg 1,4-DCB-Eq and 174.1 kg 1,4-DCB-Eq for FE and ME, respectively. SC-A slightly reduced these to 138.7 kg 1,4-DCB-Equation (−5%) and 165.8 kg 1,4-DCB-Equation (−5%), but SD-A achieved only marginal improvements, with 141.8 kg 1,4-DCB-Equation (−3%) for FE and 169.1 kg 1,4-DCB-Equation (−3%) for ME. This behavior is attributed to the high energy demand of silicon production, which becomes more prominent when the functional unit is the electrode mass. For TE, the impacts were 167.5 kg 1,4-DCB-Eq for G-A, 151.9 kg 1,4-DCB-Equation (−9%) for

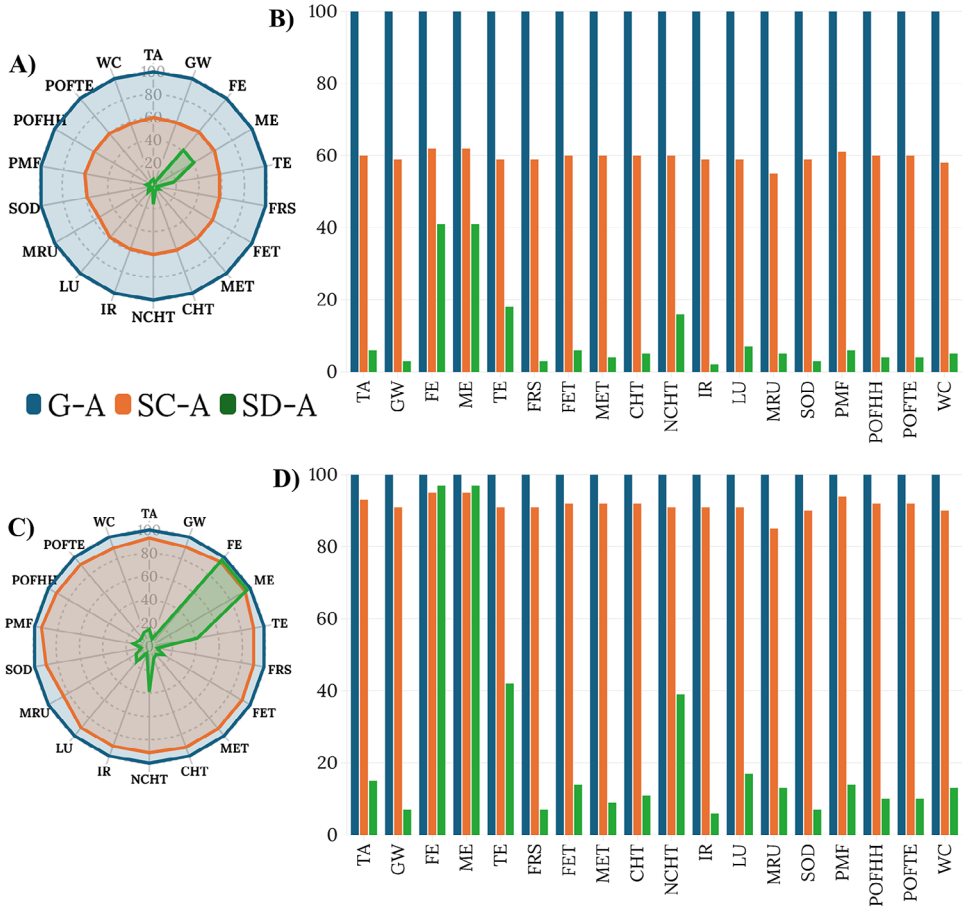


**FIGURE 6** | Graphical representation of the percentage reduction along the impact categories for the two FUs: (A) Radial diagram for 1 Ah; (B) Histogram for 1 Ah; (C) Radial diagram for 1 kg; (D) Histogram for 1 kg.

SC-A, and a significantly lower 70.7 kg 1,4-DCB-Equation (−58%) for SD-A

FRS, also reflects the advantages of silicon-dominant electrodes: G-A had the value of 51 kg oil-Eq, the SC-A the value of 46 kg oil-Eq and the SD-A the value of 3 kg oil-Eq. The percentage reduction of SC-A is 9% and for the SD-A the 93%. Considering these values, it is evident that the contribution of the SBR is important for the G-A and SC-A, and its absence led to a dramatical decrease of resource use in the case of the SD-A.

In summary, these results indicate that the environmental benefits of silicon are more evident when assessed with performance-based metrics (e.g., 1 Ah) rather than mass-based metrics (e.g., 1 kg). Nevertheless, the silicon-dominant anode achieves substantial reductions across most impact categories, underscoring its potential to lower the environmental footprint of anode production, particularly when combined with optimized manufacturing processes and cleaner energy mixes.

### 3.3 | European Supply Chain Impact on the Anodes Production

The sensitivity analysis was performed to evaluate how sourcing all materials within Europe would affect the environmental impacts of anode production. In the baseline scenario, which reflects the current situation, most of the key inputs, including graphite, silicon composite, carbon black, binders such as CMC and SBR, as well as current collectors and other cell components, are imported from outside Europe, primarily from China. In the prospective scenario, all these materials were assumed to be supplied by European producers.

As already described in the sub-chapter “Sensitivity analysis” of the previous section, transportation modelling was carried out using the Ecoinvent database, which incorporates data from Eurostat. This database classifies goods into categories and assigns average transport distances, divided among inland waterways, rail, and lorry. For this study, the RER-08 category was used for chemicals such as graphite, silicon composite, carbon black, CMC, and SBR, while the RER-10 category was applied to metals, including copper and aluminium current collectors as well as stainless steel components.

One of the limitations related to this sensitivity analysis was to consider only the transportation stage, modifying the input parameters in the software, while the material’s production processes were kept the same. This choice was related to the great complexity that lies behind this process where the change in a single parameter can influence all the results. Even with this limitation, the results highlight the importance of supply

**TABLE 5** | Life cycle environmental impacts calculated for the actual production of 1 kg of different types of anodes and relative percentage reduction, considering the graphite anode as the baseline.

| Impact category | Unit | Results per 1 kg of production | | |
|---|---|---|---|---|
| | | G-A | SC-A | SD-A |
| Acidification: terrestrial (TA) | kg $SO_2$-Eq | 0.364269 | 0.337052 | 0.05516 |
| Climate change (GW) | kg $CO_2$-Eq | 157.114 | 143.517 | 11.472 |
| Ecotoxicity: freshwater (FE) | kg 1,4-DCB-Eq | 145.646 | 138.696 | 141.823 |
| Ecotoxicity: marine (ME) | kg 1,4-DCB-Eq | 174.084 | 165.754 | 169.142 |
| Ecotoxicity: terrestrial (TE) | kg 1,4-DCB-Eq | 167.461 | 151.914 | 70.7398 |
| Energy resources: non-renewable, fossil (FRS) | kg oil-Eq | 50.7658 | 46.2434 | 3.373183 |
| Eutrophication: freshwater (FET) | kg P-Eq | 0.038747 | 0.035764 | 0.005315 |
| Eutrophication: marine (MET) | kg N-Eq | 0.003539 | 0.003251 | 0.00031 |
| Human toxicity: carcinogenic (CHT) | kg 1,4-DCB-Eq | 14.4573 | 13.2835 | 1.564266 |
| Human toxicity: non-carcinogenic (NCHT) | kg 1,4-DCB-Eq | 118.786 | 108.662 | 46.4998 |
| Ionizing radiation (IR) | kBq Co-60-Eq | 20.9946 | 19.0947 | 1.163817 |
| Land use (LU) | $m^2$*a crop-Eq | 3.328147 | 3.017472 | 0.555877 |
| Material resources: metals/minerals (MRU) | kg Cu-Eq | 1.918673 | 1.623064 | 0.24521 |
| Ozone depletion (SOD) | kg CFC-11-Eq | 7.08E-05 | 6.39E-05 | 5.14E-06 |
| Particulate matter formation (PMF) | kg $PM_{2.5}$-Eq | 0.140885 | 0.13186 | 0.019484 |
| Photochemical oxidant formation: human health (POFHH) | kg $NO_x$-Eq | 0.245958 | 0.226336 | 0.024792 |
| Photochemical oxidant formation: terrestrial ecosystems (POFTE) | kg $NO_x$-Eq | 0.262762 | 0.241633 | 0.026224 |
| Water use (WC) | $m^3$ | 2.131465 | 1.913731 | 0.278077 |

chain localization. A fully European scenario would reduce the environmental burden of transportation due to shorter distances and would also indirectly benefit from the European electricity mix, which includes a significantly higher share of renewable energy compared to China. This aspect becomes particularly relevant for energy-intensive materials such as silicon, where the environmental performance improves considerably when production relies on cleaner energy sources.

Although the variations in impacts may appear modest given the small material quantities involved in this study, the analysis confirms that supply chain choices can still influence results even at the laboratory scale. A hypothetical scale-up to an industrial level, where material flows are substantially larger, the effect of adopting a European supply chain could be more significant. Overall, the findings suggest that improving domestic supply chains could substantially improve the environmental sustainability of lithium-ion battery production in Europe.

Figure 7 shows a graphical representation of materials, processes, and transportation (each with its own unit of measure), normalized to the production of a single laminate for the different chemistries. The ultimate goal is to enable a more direct comparison between materials, processes, and transportation, and their relative correlations, with the current global supply chain illustrated on the left and the theoretical European supply chain on the right. The materials involved in the mixing step graphite, silicon composite or silicon, conductive additive, binders and water are inserted considering their amount (grams) as the width factor of the cake graph. These quantities remain constant when comparing the global and European supply chains; therefore, any variation in the width of these segments is only due to adjustments in other parameters. The time required, expressed in hours for each production step is also represented as a width factor, providing a clearer visualization of the significant reduction in processing time for the silicon-dominant anode compared to the other two types. This visualization highlights that the reduction in processing time is directly linked to lower electricity consumption. As a result, when considering the European supply chain, transportation becomes a comparatively more influential factor in the overall environmental impact of the production process.

Table 6 reports a comparison between the values calculated for the actual production and those obtained for the theoretical European production using 1 Ah as the functional unit. The values for the 1 kg FU are reported in Table S6, with results that are in line with the other FU. The percentage reductions for each chemistry are shown in italics, allowing for a clear comparison

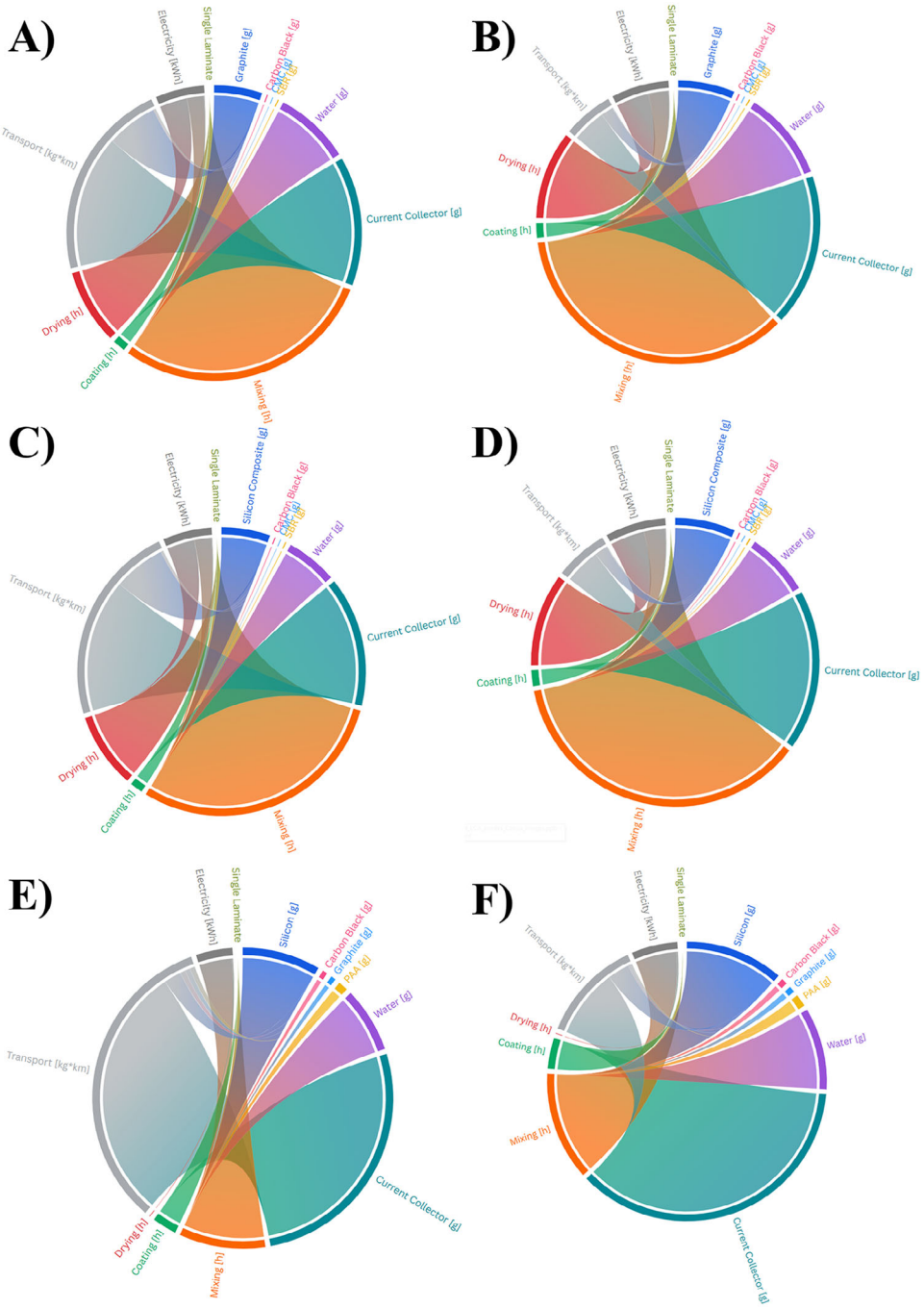


**FIGURE 7** | Comparison of the production of a single laminate considering the Actual Global supply chain in the left: (A) Graphite; (C) Silicon Composite; (E) Silicon-dominant. The theoretical European supply chain is represented on the right of the image (B) Graphite; (D) Silicon Composite; (F) Silicon-dominant.

between the different anode types. Although the absolute values are relatively small, the differences between the chemistries remain evident, and these trends are graphically represented in Figure 8.

As shown in Figure 8, several categories clearly reduced the impacts with the adoption of a European supply chain. For instance, in the case of GW, the European supply chain reduces $CO_2$ emissions across all chemistries. This positive effect is mainly due to the reduction in the use of coal as an energy source in Europe, replaced by a higher share of renewable energy. A similar trend is observed for FRS, where the reduction is linked to more sustainable electricity production that minimizes the use of fossil fuel resources.

However, not all categories benefit from the change of localization. For FE and ME, impacts are generally higher in the European scenario. This is mainly due to less efficient mining and production activities within the region, which require more energy-intensive technologies and chemicals, causing an increase in emissions in these categories. The same reason can apply to MET, which is also influenced by mining activities; in this case,

**TABLE 6** | Comparison between life cycle environmental impacts calculated for the Global Actual Production and Theoretical European supply chain production of 1Ah of different chemistries, in italic are reported the percentage variation.

| Impact category | Global Actual Production | | | Theoretical European Production | | | | | |
|---|---|---|---|---|---|---|---|---|---|
| | G-A | SC-A | SD-A | G-A | | SC-A | | SD-A | |
| TA | 0.003093 | 0.001862 | 0.000196 | 0.003090 | −0.097 | 0.001848 | −0.752 | 0.000195 | −0.510 |
| GW | 1.334065 | 0.792770 | 0.040852 | 1.333506 | −0.042 | 0.788361 | −0.556 | 0.040387 | −1.138 |
| FE | 1.236692 | 0.766139 | 0.505038 | 1.236895 | 0.016 | 0.766252 | 0.015 | 0.505116 | 0.015 |
| ME | 1.478156 | 0.915604 | 0.602320 | 1.478408 | 0.017 | 0.915734 | 0.014 | 0.602414 | 0.016 |
| TE | 1.421925 | 0.839153 | 0.251907 | 1.427293 | 0.378 | 0.839641 | 0.058 | 0.248498 | −1.353 |
| FRS | 0.431055 | 0.255443 | 0.012012 | 0.431001 | −0.013 | 0.254559 | −0.346 | 0.011911 | −0.841 |
| FET | 0.000329 | 0.000198 | 1.89E-05 | 0.000329 | 0.000 | 0.000198 | 0.000 | 1.89E-05 | −0.100 |
| MET | 3.00E-05 | 1.80E-05 | 1.10E-06 | 3.01E-05 | 0.126 | 1.81E-05 | 0.635 | 1.11E-06 | 1.070 |
| CHT | 0.122757 | 0.073376 | 0.005570 | 0.122719 | −0.031 | 0.072766 | −0.831 | 0.005516 | −0.969 |
| NCHT | 1.008620 | 0.600234 | 0.165588 | 1.009423 | 0.080 | 0.597445 | −0.465 | 0.165731 | 0.086 |
| IR | 0.178266 | 0.105477 | 0.004144 | 0.178527 | 0.146 | 0.108485 | 2.852 | 0.004239 | 2.292 |
| LU | 0.028259 | 0.016668 | 0.001979 | 0.028271 | 0.042 | 0.016707 | 0.234 | 0.001973 | −0.303 |
| MRU | 0.016292 | 0.008966 | 0.000873 | 0.016306 | 0.086 | 0.008977 | 0.123 | 0.000870 | −0.344 |
| SOD | 6.01E-07 | 3.53E-07 | 1.83E-08 | 6.01E-07 | −0.007 | 3.52E-07 | −0.176 | 1.82E-08 | −0.754 |
| PMF | 0.001196 | 0.000728 | 6.94E-05 | 0.001194 | −0.167 | 0.000712 | −2.198 | 6.83E-05 | −1.541 |
| POFHH | 0.002088 | 0.001250 | 8.83E-05 | 0.002087 | −0.048 | 0.001234 | −1.280 | 8.78E-05 | −0.570 |
| POFTE | 0.002231 | 0.001335 | 9.34E-05 | 0.002230 | −0.045 | 0.001318 | −1.273 | 9.28E-05 | −0.589 |
| WC | 0.018098 | 0.010571 | 0.000990 | 0.018100 | 0.011 | 0.010603 | 0.303 | 0.000991 | 0.101 |

using recycled materials could significantly reduce the associated emissions [9].

For IR, the higher impact in Europe is directly related to the greatest share of nuclear power in the European energy mix, which is the primary driver of this category [9]. Regarding the ecotoxicity categories, it is notable that all anode chemistries generally show relatively small impacts, with the exception of TE, where the silicon-dominant anodes show a substantial improvement compared to the other chemistries.

### 3.4 | Uncertainties Evaluation Through Monte Carlo Simulations

A sensitivity analysis was conducted on GW impact category to better understand the impact of the uncertainties during the calculations. For each case analyzed, three independent MCS runs with 10,000 iterations were performed, only one of them is presented here. The uncertainties in the systems were derived from secondary data, as these inputs could not be directly controlled during the production process.

For electricity contribution, the power demand of each piece of equipment and the corresponding operating times were precisely known, enabling accurate calculation of energy use at each process step. However, no specific information was available regarding the type of electricity supply, hence, the Pedigree matrix was built using the lowest uncertainty values in each category. For transportation, the available information was more limited than for electricity consumption. In this case, the Pedigree matrix was constructed using data from comparable processes in the Ecoinvent database. Consequently, uncertainties related to transport were higher than those for electricity.

According to the work of Gao et al., the coefficient of variability was calculated from the MCS results. In this study, the coefficients were consistently less than half of those reported in the cited work, with the lowest value observed for SD-A [37]. This result is attributed to the lower level of uncertainty throughout the SD-A production process, which was carefully monitored and controlled.

Table 7 reports the results for the production of 1Ah, comparing all the three anode types under the actual global production process and the theoretical European supply chain scenario. In all cases, the mean and median values deviated only negligibly (at the third or even fourth decimal place) from the base case previously calculated without accounting for uncertainties. For the actual 1Ah production, the coefficient of variability was 2.46 for G-A, 2.47 for SC-A and 2.04 for SD-A. The particularly low value for SD-A reflects its lower electricity consumption during production and the reduced uncertainty in transportation data, since the silicon was sourced from E-Magy Company, located in the Netherlands, allowing for more precise transport modelling. For each condition, three independent MCS calculations were performed confirming the reproducibility of the method.

The graphical representation of the data distribution related to the actual production process of 1Ah is shown in Figure 9.

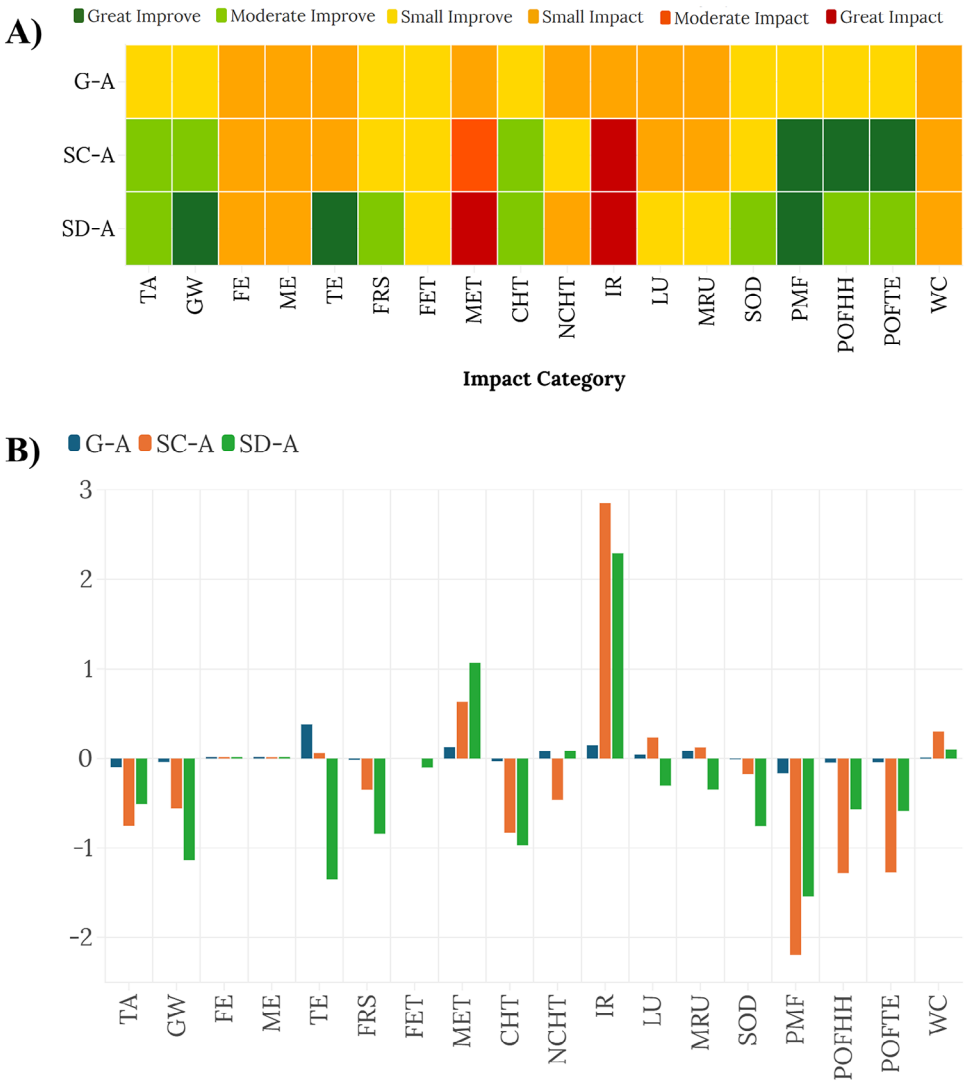


**FIGURE 8** | Comparison between the Actual Global supply chain and the European Theoretical supply chain. (A) Graphical representation; (B) Percentage comparison: the bars below 0 are associated to a reduction of the impacts, while the bars above 0 are associated to an increase of the impacts.

**TABLE 7** | Comparison of the statistical evaluation of GW impact distribution between the actual production and the European theoretical supply chain for the production of 1Ah of the different types of anodes.

| | | Actual Global Production – 1Ah | | | European Supply Chain – 1Ah | | |
|---|---|---|---|---|---|---|---|
| | Unit | G-A | SC-A | SD-A | G-A | SC-A | SD-A |
| Trials | — | 10 000 | 10 000 | 10 000 | 10 000 | 10 000 | 10 000 |
| Base Case | kg $CO_2$-Eq | 1.3341 | 0.7928 | 0.0409 | 1.3335 | 0.7884 | 0.0404 |
| Mean | kg $CO_2$-Eq | 1.3338 | 0.793 | 0.0409 | 1.3346 | 0.7883 | 0.0404 |
| Median | kg $CO_2$-Eq | 1.3306 | 0.7911 | 0.0408 | 1.3313 | 0.7863 | 0.0403 |
| Standard Deviation | kg $CO_2$-Eq | 0.0328 | 0.0196 | 0.0008 | 0.0334 | 0.0198 | 0.0008 |
| 5% percentile | kg $CO_2$-Eq | 1.2856 | 0.7644 | 0.0396 | 1.2857 | 0.7596 | 0.0391 |
| 95% percentile | kg $CO_2$-Eq | 1.3914 | 0.8279 | 0.0423 | 1.3941 | 0.8231 | 0.0419 |
| Coefficient of variability | % | 2.4621 | 2.4755 | 2.0407 | 2.5028 | 2.5149 | 2.083 |
| Minimum | kg $CO_2$-Eq | 1.2422 | 0.7394 | 0.0382 | 1.2267 | 0.7306 | 0.0376 |
| Maximum | kg $CO_2$-Eq | 1.5116 | 0.9064 | 0.0472 | 1.4994 | 0.9015 | 0.0444 |

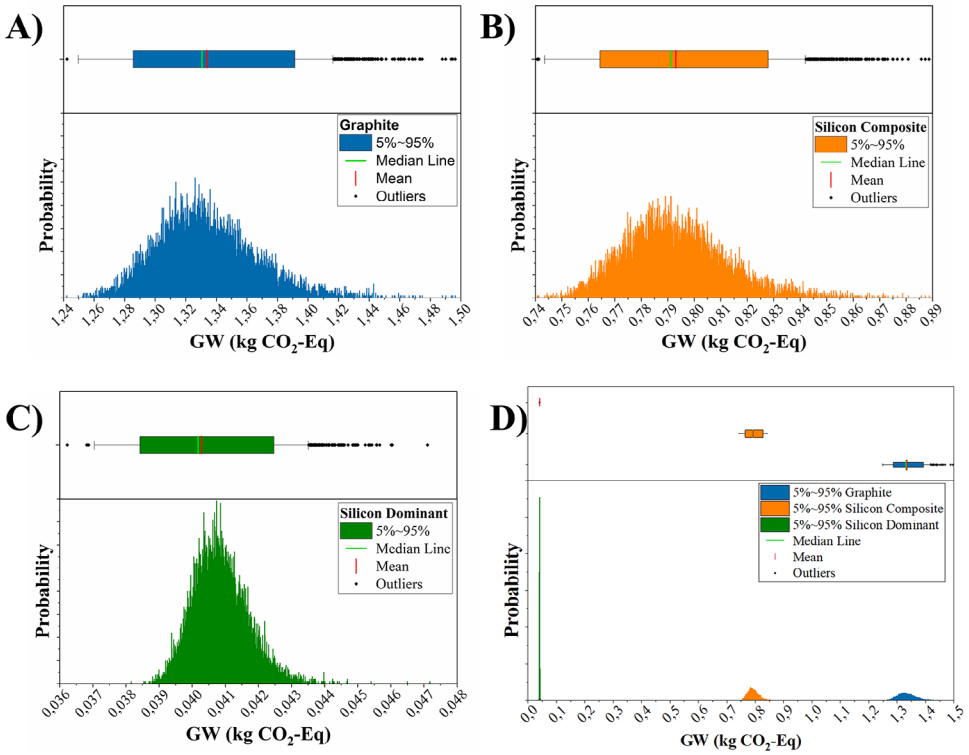


**FIGURE 9** | Gaussian distribution of 10,000 MCS for the actual production of 1Ah, the impact category presented is the GW. For all the graphs, in the top diagram, the box plot with mean and median lines and relative outliers are reported, in the bottom diagram the Gaussian-shaped histogram is presented. (A) G-A; (B) SC-A; (C) SD-A; (D) Comparison of the three different types of anodes produced.

For all the anode types, the median (green line) and mean (red line) values closely match the best-case value, with only minimal deviations arising from the non-symmetric nature of the uncertainty distributions. The G-A (Figure 9A) and SC-A (Figure 9B) exhibited relatively broad, Gaussian-like distributions, whereas SD-A (Figure 9C) showed a narrower but less symmetric Gaussian-like distribution. A direct comparison of the three distributions is provided in Figure 9D, highlighting the narrower spread of SD-A relative to the G-A and SC-A.

A similar behavior was observed for the actual production of 1 kg of anodes (Figure S4), as for the 1 Ah distributions, also for the 1 kg functional unit is characterized by the SD-A with the narrowest distribution. Compared to the 1 Ah FU, in this second case, the G-A and SC-A distributions are closer, meaning that their impacts are more similar to this FU. The results obtained for the MCS for 1 kg are reported in Table S7 with the same procedure as the previous calculation. The coefficients of variability are in line within the two FU.

The same MCS calculations were performed for the theoretical European supply chain scenario, the results for the 1 Ah FU are reported in Figure S5, while the results for the 1 kg FU are in Figure S6.

To ensure a proper comparison among the three types of anodes, the comparison between the actual global production and the theoretical European supply chain scenarios, is reported in Figure 10, for the G-A, SC-A and SD-A, respectively. Overall, the distribution shapes are similar across the three chemistries, each maintaining its characteristic non-symmetric profile. In Figure 10A, which compares the MCS results for G-A, the different supply chains show minimal influence on $CO_2$ emissions for this type of production. By contrast, Figure 10B,C displays a more pronounced reduction in emissions for SC-A and SD-A, where the distribution peaks for the European supply chain are shifted toward lower values, confirming the environmental advantages of localized sourcing for these chemistries.

The outcomes of the MCS further support the findings obtained from the deterministic analysis of the environmental impacts. The narrow distributions observed, particularly for the SD-A, highlight the robustness and reliability of the results despite the inherent uncertainties associated with secondary data. The lower variability for SD-A compared to G-A and SC-A confirms that careful control of the production process and more precise knowledge of material sourcing, such as the local European production of silicon, help minimize uncertainties. Furthermore, the shift of the emission distributions toward lower values in the European supply chain scenario reinforces the conclusion that localized production, supported by a cleaner electricity mix and shorter transportation distances, can substantially reduce the environmental impacts of SD-A. These findings highlight the importance of coupling process optimization with regionalized supply chains to further reduce the carbon footprint of advanced lithium-ion battery anodes.

### 3.5 | Endpoint Impact Categories

To provide a more comprehensive evaluation of the environmental impacts, the same data previously analyzed at the midpoint

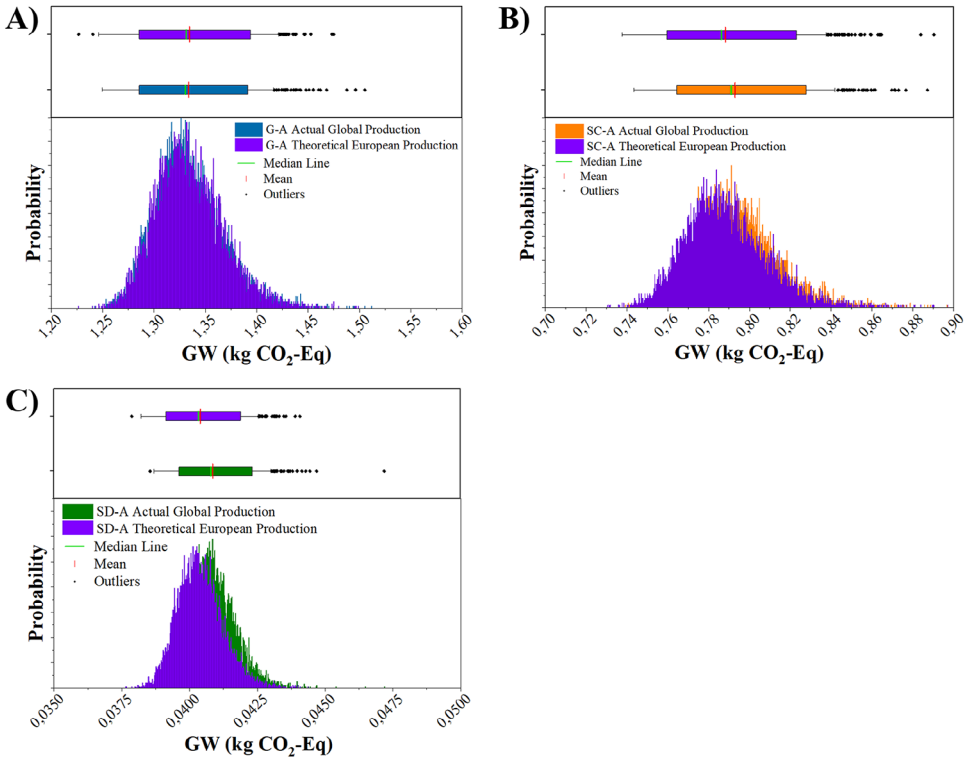


**FIGURE 10** | Comparison between the MCS performed for the Actual Global Production and the Theoretical European Production: (A) Graphite; (B) Silicon Composite; (C) Silicon-dominant.

**TABLE 8** | Values of Endpoint categories for the production of 1 Ah and 1 kg of anodes considering actual global production.

| | Global Actual Production | | | | | |
|---|---|---|---|---|---|---|
| | Results per 1 Ah of production | | | Results per 1 kg of production | | |
| **Endpoint Category** | **G-A** | **SC-A** | **SD-A** | **G-A** | **SC-A** | **SD-A** |
| Ecosystem quality [species.yr] | 6.422E-09 | 3.846E-09 | 6.271E-10 | 7.563E-07 | 6.962E-07 | 1.761E-07 |
| Human health [DALYs] | 2.671E-06 | 1.599E-06 | 1.401E-07 | 3.146E-04 | 2.895E-04 | 3.933E-05 |
| Natural resources [USD 2013] | 0.141 | 0.083 | 0.004 | 16.628 | 15.090 | 1.100 |

level were also assessed using the ReCiPe 2016 Endpoint (H) method. This approach aggregates the 18 midpoint impact categories into three broader damage categories: Ecosystem Quality, Human Health, and Natural Resources, thus enabling a higher-level interpretation of the results.

In Table 8 the endpoint impact values for the actual global production of 1 Ah and 1 kg are reported, considering that most of the materials used for the anode's preparation are sourced outside Europe. The results of this study are consistent with the findings reported by Li et al. [42], showing that the Natural Resources category has the highest contribution. This is mainly driven by the extraction of multiple materials, such as copper for the current collectors and coal for electricity generation, which dominate the impacts throughout this damage pathway.

In Table 9 are reported the endpoint impact values for the Theoretical European Production, considering the 1Ah and 1 kg as functional units. As expected, the reductions compared to the global supply chain are relatively small across most categories. However, an interesting trend emerges for Natural Resources: for both the 1 Ah and 1 kg functional units, G-A and SC-A exhibit a slight increase in impacts, whereas only SD-A shows a modest decrease. This behavior can be attributed to the relative scarcity of certain raw materials in Europe, highlighting the need for improved recycling strategies to strengthen the resource supply chain. For the other categories, no significant improvements are observed for G-A under the European scenario, while SC-A and SD-A show small but measurable reductions, reflecting the combined effect of shorter transportation routes and a cleaner energy mix.

**TABLE 9** | Values of Endpoint categories for the production of 1 Ah and 1 kg of anodes considering the theoretical European supply chain.

| Endpoint Category | Theoretical European Supply Chain | | | | | |
|---|---|---|---|---|---|---|
| | Results per 1 Ah of production | | | Results per 1 kg of production | | |
| | G-A | SC-A | SD-A | G-A | SC-A | SD-A |
| Ecosystem quality [species.yr] | 6.420E-09 | 3.830E-09 | 6.254E-10 | 7.561E-07 | 6.933E-07 | 1.756E-07 |
| Human health [DALYs] | 2.669E-06 | 1.582E-06 | 1.388E-07 | 3.143E-04 | 2.865E-04 | 3.898E-05 |
| Natural resources [USD 2013] | 0.141 | 0.083 | 0.004 | 16.632 | 15.092 | 1.094 |

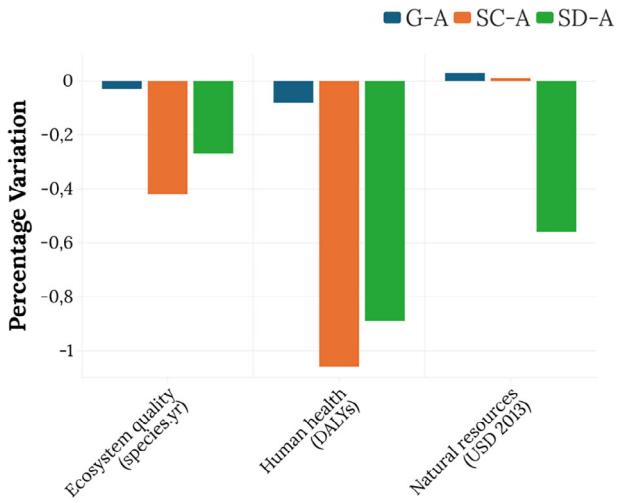


**FIGURE 11** | Percentage variation of the European supply chain compared to the actual global production for the Endpoint categories.

The percentage variation between the actual global production (Table 8) and the theoretical European supply chain (Table 9) are summarized in Figure 11. In line with the previous observations, the localized supply chain effectively reduces some impacts, especially those related to the ecosystem quality and human health sector, for all the anode types, but in different amounts. However, the scarcity of natural resources in Europe represents a drawback of this supply chain, leading to increased impacts in this category for G-A and SC-A, whereas SD-A remains more resilient and emerges as the more sustainable option.

Overall, the endpoint analysis confirms the trends already identified in the midpoint results. SD-A consistently demonstrates improved performance, with significant reductions in resource depletion and health-related damage categories when assessed on a performance basis. The relatively small differences observed in the European supply chain scenario suggest that the environmental benefits of localization are more pronounced in categories strongly influenced by transportation and electricity generation. These findings emphasize the importance of coupling material efficiency with regional supply strategies and recycling improvements to further enhance the sustainability of advanced anode chemistries.

## 4 | Final Remarks and Conclusion

The LCA performed in this study quantified the environmental impacts for the production of three different chemistry anodes (graphite, silicon composite and silicon-dominant) for the application in LIBs field. Graphite was considered as the baseline, being the most commercialized type of anode; silicon composite represented the emerging commercial option while the silicon-dominant configuration was regarded as the future innovative technology. Further LCAs should be conducted on full-cell configuration, coupling these different anodes with a cathode to better simulate commercial batteries and adopting other functional units such as the widely used 1 kWh.

Consistent with previous studies, the use of innovative materials with high silicon content showed positive effect not only on energy density but also on production sustainability, due to improved performance and processability. In particular, the SD-A achieved up to a 97% reduction in $CO_2$ emissions compared with graphite electrodes. A similar trend is expected under large-scale production, where enhanced process efficiency could further reduce waste generation and resource consumption. However, silicon production in all its forms remains energy and chemical intensive. Accordingly, developing less energy demanding processes and relying on renewable electricity sources are crucial to improving the sustainability of the supply chain.

In a global context dominated by Chinese manufacturing, the European supply chain modeled in this study offers clear sustainability advantages, primarily due to the higher share of renewable electricity and shorter transportation routes. Nevertheless, the lack of specific materials in the Ecoinvent database, such as silicon composite (approximately 10% Si), and the outdated nature of some datasets, for instance, CMC data from the 1990s, limit the accuracy of the current representation. Greater industrial transparency and data sharing would substantially improve life cycle inventories, enabling faster progress toward sustainable battery manufacturing.

The MCS conducted confirmed that uncertainty is inherent even when the model relies entirely on primary data. However, higher quality datasets lead to reduced variability; in particular, knowing the exact production location of silicon for the SD-A decreased the coefficient of variability compared with G-A and SC-A.

The results also demonstrate that restricting the LCA to the carbon footprint, considering only the GW category, is insufficient to assess process sustainability. Multiple impact categories, including TA, FRS, MRU, and WC, must be analyzed to obtain a comprehensive evaluation and to determine whether the overall outcome is beneficial.

Finally, endpoint results indicated that the natural resources damage category is the most affected in anode production for LIB applications. Hence, circular economy strategies, such as second use, recycling, and material recovery, should be further developed to mitigate these impacts and strengthen the long-term sustainability of the sector.


### Acknowledgements

Elisa Ravesio acknowledges support from the PNRR-NGEU project, funded by the Italian Ministry of University and Research (MUR) under Decree DM 352/2022. The authors also thank G.D. S.p.A. and the Coesia Engineering Center for providing technical support, access to research facilities, and valuable discussions that contributed to this work.

Open access publishing facilitated by Politecnico di Torino, as part of the Wiley - CRUI-CARE agreement.


### Conflicts of Interest

The authors declare no conflicts of interest.

### Data Availability Statement

The data that support the findings of this study are available from the corresponding author upon reasonable request.

### References


1. "Europe Now Has 30 EV Battery Gigafactories in Operation," accessed September 15, 2025, https://electricdrives.tv/europe-now-has-30-ev-battery-gigafactories-in-operation/.

2. S. M. Pinto, R. A. Dos Reis, C. C. Fraga, and E. J. Lourenço, "Life Cycle Sustainability Assessment Strategy for NMC Lithium-Ion Battery," *Procedia CIRP* 135 (2025): 679–684, https://doi.org/10.1016/j.procir.2024.12.076.

3. A. Mauger, H. Xie, and C. M. Julien, "Composite Anodes for Lithium-Ion Batteries: Status and Trends," *AIMS Materials Science* 3 (2016): 1054–1106, https://doi.org/10.3934/matersci.2016.3.1054.

4. Y. Gao, Z. Pan, J. Sun, Z. Liu, and J. Wang, "High-Energy Batteries: Beyond Lithium-Ion and Their Long Road to Commercialisation," *Nano-Micro Letters* 14, no. 1 (2022): 1–49, https://doi.org/10.1007/S40820-022-00844-2.

5. J. C. Barbosa, R. S. Pinto, J. P. Serra, et al., "Batteries and Sustainability: The Relevance of Life Cycle Assessment," *Sustainable Energy Technologies and Assessments* 82 (2025): 104488, https://doi.org/10.1016/j.seta.2025.104488.

6. F. Wang, C. Intrator, N. Salopek, and C. Yuan, *An Environmental Sustainability Analysis Tool for Next Generation Lithium Ion Batteries of Electric Vehicles* (Procedia CIRP), 489–494, https://doi.org/10.1016/j.procir.2022.02.081.

7. Vijaya, P. K. Nema, P. Kalita, and R. Thangavel, "Life Cycle Assessment of Lithium-ion Batteries With Carbon-coated Silicon-graphite Composite Anodes: Impact of Silicon Content on Cradle-to-gate Environmental Footprint," *Environmental Science and Pollution Research* (2025): 1–15, https://doi.org/10.1007/s11356-025-36270-1.

8. B. Li, J. Li, and C. Yuan, "Life Cycle Assessment of Lithium Ion Batteries With Silicon Nanowire Anode for Electric Vehicles," in *Proceedings of the International Symposium on Sustainable Systems and Technologies* (Sustainable Conoscente Network, 2013), https://doi.org/10.6084/m9.figshare.805147.

9. M. Lavigne Philippot, D. Costa, G. Cardellini, et al., "Life Cycle Assessment of a Lithium-ion Battery With a Silicon Anode for Electric Vehicles," *Journal of Energy Storage* 60 (2023): 106635, https://doi.org/10.1016/j.est.2023.106635.

10. Z. Wu and D. Kong, "Comparative Life Cycle Assessment of Lithium-Ion Batteries With Lithium Metal, Silicon Nanowire, and Graphite Anodes," *Clean Technologies and Environmental Policy* 20 (2018): 1233–1244, https://doi.org/10.1007/s10098-018-1548-9.

11. B. Li, X. Gao, J. Li, and C. Yuan, "Life Cycle Environmental Impact of High-Capacity Lithium Ion Battery With Silicon Nanowires Anode for Electric Vehicles," *Environmental Science & Technology* 48 (2014): 3047–3055, https://doi.org/10.1021/es4037786.

12. M. J. Lain, Y. Wu, A. Smith, S. Bolloju, S. R. Coles, and L. F. J. Piper, "A Comparative Life Cycle Assessment of Different Lithium Ion Anode Manufacturing Routes Based on Graphite and/or Silicon," *Sustainable Materials and Technologies* 45 (2025): 01609, https://doi.org/10.1016/j.susmat.2025.e01609.

13. Y. Deng, L. Ma, T. Li, J. Li, and C. Yuan, "Life Cycle Assessment of Silicon-Nanotube-Based Lithium Ion Battery for Electric Vehicles," *ACS Sustainable Chemistry & Engineering* 7 (2019): 599–610, https://doi.org/10.1021/acssuschemeng.8b04136.

14. M. Erakca, M. Baumann, W. Bauer, et al., "Energy Flow Analysis of Laboratory Scale Lithium-ion Battery Cell Production," *Iscience* 24 (2021): 102437, https://doi.org/10.1016/j.isci.2021.102437.

15. F. Scrucca, A. Presciutti, G. Baldinelli, G. Barberio, L. Postrioti, and C. Karaca, "Life Cycle Assessment of Li-Ion Batteries for Electric Vehicles: A Review Focused on the Production Phase Impact," *Journal of Power Sources* 639 (2025): 236703, https://doi.org/10.1016/j.jpowsour.2025.236703.

16. M. Erakca, S. P. Bautista, S. Moghaddas, et al., "Closing Gaps in LCA of Lithium-ion Batteries: LCA of Lab-scale Cell Production With New Primary Data," *Journal of Cleaner Production* 384 (2023): 135510, https://doi.org/10.1016/j.jclepro.2022.135510.

17. E. A. Olivetti, G. Ceder, G. G. Gaustad, and X. Fu, "Lithium-Ion Battery Supply Chain Considerations: Analysis of Potential Bottlenecks in Critical Metals," *Joule* 1 (2017): 229–243, https://doi.org/10.1016/j.joule.2017.08.019.

18. L. Boon-Brett, F. Di Persio, N. Lebedeva, and M. Steen, *EU Competitiveness in Advanced Li-ion Batteries for E-Mobility and Stationary Storage Applications: Opportunities and Actions* (JRC Science Hub, 2017), 1–49, https://doi.org/10.2760/75757.

19. "Research & Innovation Roadmap 2023 – Batteries Europe," accessed October 28, 2025,, https://batterieseurope.eu/results/technology-roadmap/researchandinnovationroadmap-2023/.

20. F. Maroni, M. Spreafico, A. Schönecker, M. Wohlfahrt-Mehrens, and M. Marinaro, "Near-Zero Volume Expansion Nanoporous Silicon as Anode for Li-Ion Batteries," *Journal of The Electrochemical Society* 169 (2022): 080506, https://doi.org/10.1149/1945-7111/ac8628.

21. A. Osmanpour, J. Poen, V. Ruiz, K. Tariq, and W. P. Kalisvaart, "Stable, Scalable Micron-Sized Porous Silicon for High Energy Density Li-Ion Batteries," *Batteries & Supercaps* 8 (2025): 202500500, https://doi.org/10.1002/batt.202500500.

22. W. J. Legerstee, T. Noort, T. K. van Vliet, H. Schut, and E. M. Kelder, "Characterisation of Defects in Porous Silicon as an Anode Material Using Positron Annihilation Doppler Broadening Spectroscopy," *Applied Nanoscience* 12 (2022): 3399–3408, https://doi.org/10.1007/s13204-022-02550-2.

23. L. A. W. Ellingsen, G. Majeau-Bettez, B. Singh, A. K. Srivastava, L. O. Valøen, and A. H. Strømman, "Life Cycle Assessment of a Lithium-

Ion Battery Vehicle Pack," *Journal of Industrial Ecology* 18 (2014): 113–124, https://doi.org/10.1111/jiec.12072.

24. M. Philippot, G. Alvarez, E. Ayerbe, J. Van Mierlo, and M. Messagie, "Eco-Efficiency of a Lithium-Ion Battery for Electric Vehicles: Influence of Manufacturing Country and Commodity Prices on GHG Emissions and Costs," *Batteries* 5 (2019): 23, https://doi.org/10.3390/batteries5010023.

25. D. Paul, V. Pechancová, N. Saha, et al., "Life Cycle Assessment of Lithium-Based Batteries: Review of Sustainability Dimensions," *Renewable and Sustainable Energy Reviews* 206 (2024): 114860, https://doi.org/10.1016/j.rser.2024.114860.

26. N. Hayagan, C. Aymonier, L. Croguennec, et al., "Direct Recycling Process Using Pressurized CO2 for Li-Ion Battery Positive Electrode Production Scraps," *ACS Sustainable Chemistry & Engineering* 13 (2024): 105–118, https://doi.org/10.1021/acssuschemeng.4C05591.

27. P. Nuss and K. H. Gardner, "Attributional Life Cycle Assessment (ALCA) of Polyitaconic Acid Production From Northeast US Softwood Biomass," *The International Journal of Life Cycle Assessment* 18 (2013): 603–612, https://doi.org/10.1007/s11367-012-0511-y.

28. A. Jinasena, O. S. Burheim, and A. H. Strømman, "A Flexible Model for Benchmarking the Energy Usage of Automotive Lithium-Ion Battery Cell Manufacturing," *Batteries* 7 (2021): 14, https://doi.org/10.3390/batteries7010014.

29. M. L. Carvalho, A. Temporelli, E. Brivio, P. C. Brambilla, G. Mela, and P. Girardi, "Batteries in Motion: A Life Cycle Assessment and Critical Resource Use Analysis of Micromobility Vehicles With Primary Li-ion Battery Data," *Journal of Energy Storage* 125 (2025): 116965, https://doi.org/10.1016/j.est.2025.116965.

30. C. D. Reynolds, P. R. Slater, S. D. Hare, M. J. H. Simmons, and E. Kendrick, "A Review of Metrology in Lithium-ion Electrode Coating Processes," *Materials & Design* 209 (2021): 109971, https://doi.org/10.1016/j.matdes.2021.109971.

31. M. A. J. Huijbregts, Z. J. N. Steinmann, P. M. F. Elshout, et al., "ReCiPe2016: A Harmonised Life Cycle Impact Assessment Method at Midpoint and Endpoint Level," *The International Journal of Life Cycle Assessment* 22 (2017): 138–147, https://doi.org/10.1007/s11367-016-1246-y.

32. "Global Battery Supply Chain: Hidden Regional Trends | McKinsey," accessed September 5, 2025, https://www.mckinsey.com/features/mckinsey-center-for-future-mobility/our-insights/the-hidden-trends-in-battery-supply-and-demand-a-regional-analysis.

33. "Critical Raw Materials Act—European Commission," accessed September 2, 2025, https://single-market-economy.ec.europa.eu/sectors/raw-materials/areas-specific-interest/critical-raw-materials/critical-raw-materials-act_en#actions-under-the-critical-raw-materials-act.

34. N. B. Manjong, V. Bach, L. Usai, et al., "A Comparative Assessment of Value Chain Criticality of Lithium-ion Battery Cells," *Sustainable Materials and Technologies* 36 (2023): 00614, https://doi.org/10.1016/j.susmat.2023.e00614.

35. J. L. Popien, J. Husmann, A. Barke, et al., "Comparison of Lithium-Ion Battery Supply Chains—A Life Cycle Sustainability Assessment," *Procedia CIRP* 116 (2023): 131–136, https://doi.org/10.1016/j.procir.2023.02.023.

36. "Database—Transport—Eurostat," accessed September 2, 2025, https://ec.europa.eu/eurostat/web/transport/database.

37. B. Gao, S. Yang, and S. Peng, "Bayesian Monte Carlo-Assisted Life Cycle Assessment of Lithium Iron Phosphate Batteries Production for Electric Vehicles Under uncertainty," *Green Manufacturing Open* 2, no. n.d. (2024): 18, https://doi.org/10.20517/gmo.2024.092201.

38. S. D. Kurland, "Energy Use for GWh-scale Lithium-ion Battery Production," *Environmental Research Communications* 2 (2020): 012001, https://doi.org/10.1088/2515-7620/ab5e1e.

39. J. Zhang, X. Ke, Y. Gu, et al., "Cradle-to-Gate Life Cycle Assessment of All-Solid-State Lithium-Ion Batteries for Sustainable Design and Manufacturing," *The International Journal of Life Cycle Assessment* 27 (2022): 227–237, https://doi.org/10.1007/s11367-022-02023-2.

40. "E-magy - The Battery Industry Is On with Silicon," accessed September 6, 2025, https://e-magy.com/.

41. "Global Energy Review 2025 – Analysis—IEA," accessed October 28, 2025, https://www.iea.org/reports/global-energy-review-2025.

42. X. Li, Y. Qian, M. Xie, D. Liu, and Q. Qiao, "An Endpoint Model for Life Cycle Impact Assessment in China and Preliminary Normalization Values: A Case Study of Vehicles," *Journal of Cleaner Production* 434 (2024): 140326, https://doi.org/10.1016/j.jclepro.2023.140326.

## Supporting Information

Additional supporting information can be found online in the Supporting Information section.

**Supporting File**: adsu70398-sup-0001-SuppMat.docx.